ELSEVIER

Journal of Power Sources 68 (1997) 296–300

JOURNAL OF POWER SOURCES

High capacity carbon anode materials: structure, hydrogen effect, and stability

P. Zhou, P. Papanek, C. Bindra, R. Lee, J.E. Fischer *

Department of Materials Science and Engineering and Laboratory for Research on the Structure of Matter, University of Pennsylvania, Philadelphia, PA 19104-6272, USA

Accepted 24 September 1996

Abstract

The local structure of several disordered carbons, obtained from radial distribution function analysis of elastic neutron scattering data, consists of small isolated graphene fragments. The effect of residual hydrogen which presumably saturates the dangling bonds in low-temperature pyrolyzed materials was studied by inelastic neutron vibrational spectroscopy and computer modelling of lithiated polyaromatic hydrocarbons. We discuss the possibility of exploiting the high-pressure crystal phase LiC_2 in primary batteries, by demonstrating that trace boron substitition greatly enhances the (meta)stability of this phase at atmospheric pressure. © 1997 Elsevier Science S.A.

Keywords Carbon, Intercalation; Neutron diffraction, X-ray diffraction

1. Introduction

Li–carbon compounds overcome many of the disadvantages encountered with metallic Li anodes. The large and growing variety of carbon-based materials suggests the possibility of increasing the maximum Li/carbon ratio, in particular by using disordered carbons. Here we summarize our results on: (i) neutron diffraction and radial distribution function analysis to determine the local structure of disordered carbons; (ii) computer simulations [1] and vibrational spectroscopy directed towards elucidating the role of residual hydrogen in low-temperature pyrolyzed carbons, and (iii) prospects for stabilizing super-dense high pressure-synthesized LiC_2 for use in primary batteries [2].

2. Local structure of disordered carbons

Extensive work by Dahn et al. [3] shows that non-crystalline carbons exhibit even greater Li capacities than crystal graphite. As a first step towards a microscopic understanding of Li uptake in such materials, we measured the local structures of a variety of disordered carbons using neutron radial distribution function (RDF) analysis [4,5] and real space modeling. Representative data from two of Dahn's materials are presented; their RDF's turn out to be typical of measurements from a wide variety of disordered carbons, obtained from different precursors with different pyrolysis temperatures.

In RDF analysis, the differential correlation function $D(r)$ is obtained by Fourier-transforming the elastic structure factor $S(Q)$

$$D(r)=\frac{2}{\pi}\int_0^\infty Q[S(Q)-1]\sin(Qr)dQ=4\pi r(\rho(r)-\rho_0)$$

where $\rho(r)$ is the number of atoms per unit volume at r, ρ_0 is the average microscopic density and $Q=4\pi\sin\theta/\lambda$ is the momentum transfer. Other quantities of interest are the total correlation function $T(r)=4\pi r\rho(r)$ and the RDF $=4\pi r^2\rho(r)$, the latter being the number density at a distance r from a reference atom. For a gas, $\rho(r)=\rho_0$ at all r, thus $D(r)=0$ and the RDF is smooth and featureless. Short-range (or long-range) correlations in condensed matter produce peaks in $D(r)$, and oscillations in the RDF about the average parabola defined by the r^2 factor. Spatial resolution is limited by truncation broadening due to termination of the integral at the maximum experimentally accessible momentum transfer Q_{max}. In X-ray diffraction (XRD) Q_{max} is limited to ~ 18 Å^{-1} using Mo K_α, while electron diffraction is complicated by absorption and multiple-scattering. We used pulsed time-of-flight neutron diffraction and the glass-liquid-

* Corresponding author.

PII S0378-7753(96)02563-3

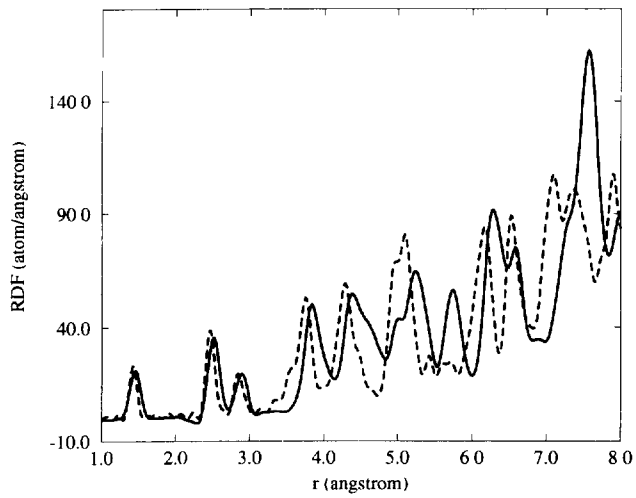

Fig 1. Neutron RDF ($4\pi r^2\rho$) of (- - -) graphite and (——) LiC_6 obtained from pulsed time-of-flight neutron diffraction

amorphous material diffractometer (GLAD) at the intense pulse neutron source (IPNS) of Argonne National Laboratory with a $Q_{max} = 45$ Å^{-1} [5].

Crystalline graphite and LiC_6 powders were studied as standards. In Fig. 1 we plot the RDF's of graphite (dashed curve) and LiC_6 (solid curve). Sharp peaks can be seen in both, corresponding to shells of atoms at well-defined distances from a reference atom. For graphite, the first peak is at 1.43 Å, corresponding to the smallest C–C distance (in-plane bond length). The first and second peak positions give the bond angle, $120 \pm 1°$. The third, the intra-hexagon distance, is 2.86 Å, twice the bond length, a signature of planar hexagons. Integrated intensities for the first three peak are 2.98, 6.09 and 3.5 atoms, respectively, in reasonable agreement with the expected values 3.0, 6.0 and 3.0. The first interlayer C–C correlation should occur at 3.35 Å with a coordination of 1, since only half the C–C pairs are eclipsed. This can be identified as a shoulder on the lower side of the fourth (in-plane) neighbor peak at 3.75 Å. The average density ρ_0, fixed by requiring the RDF to vanish below the first peak, is 2.26 g/cm^3, in excellent agreement with the handbook value 2.23 g/cm^3. All of these local observations are entirely consistent with the well-known edge-connected hexagonal network of sp^2-hybridized carbons.

Most of the RDF peaks in LiC_6 (solid curve Fig. 1) are up-shifted relative to graphite. This is due to the elongation of the near-neighbor C–C distance upon intercalation, a consequence of electron donation from Li to carbon layers — charge added to the carbon π system slightly weakens the σ bonds. Spatial correlations between heteroatoms Li and C give rise to the negative peak at 2.36 Å because the neutron scattering length of Li (natural abundance of ^{6}Li and ^{7}Li) is negative. The observed Li–C distance is consistent with intercalated interstitial Li sandwiched symmetrically between two eclipsed hexagons, which in turn is consistent with the known change in graphite layer stacking from ABAB to AαAα, where A and B represent carbon layers and α the lithium layer [6]. Similarly, the interlayer C–C shoulder at 3.35 Å is gone in LiC_6; all the carbons are now eclipsed and the interlayer spacing has increased to 3.7 Å.

The above results on crystalline prototypes give us confidence that the corresponding local information will be obtainable from disordered carbons using the same methods. In Fig. 2 we plot $D(r)$ which emphasizes the oscillations arising from short-range correlations, for two epoxy novlac resins (ENR) pyrolyzed at 650 or 1000 °C. Details of the preparation can be found in Dahn's papers, see Ref. [3]. These are denoted ENR650 (H/C = 0.24, solid curve) and ENR1000 (H/C = 0.04, dotted curve). The RDF of polycrystalline graphite is shown for comparison (upper curve). The $D(r)$'s of ENR650 and ENR1000 are quite similar, with most peaks located at the same positions as in graphite, suggesting the same bond length and angle, a hexagonal planar local motif and sp^2-hybridized carbons. The peak intensities are weaker than in graphite, the discrepancy increasing with increasing r. For the low-order peaks, this has a very simple interpretation — a significant number of edge atoms with only two neighbors. The absence of strong peaks above ~6 Å sets the approximate scale of the in-plane particle size. In Fig. 3 we compare $D(r)$ of ENR1000 (solid curve) with a model calculation assuming isolated graphene fragments 5 hexagons on a side (dotted curve). The agreement is quite satisfactory.

We conclude that carbons obtained by pyrolysis of epoxy novolac resin at temperatures from 650 to 1000 °C consist of small graphene fragments with lateral dimensions of 10 Å. The fact that these fragments are planar and the carbon atoms are sp^2-hybridized imply that the residual hydrogens are bonded to the edge atoms. Inter-graphene correlations are not

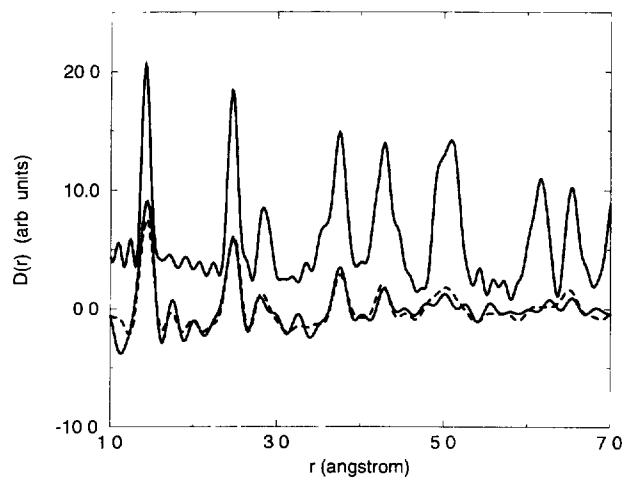

Fig 2 Differential correlation functions $D(r)$ of epoxy novolac resin pyrolyzed at (——) 650 °C ENR650 and (· · ·) 1000 °C ENR1000, and graphite (upper curve) for comparison.

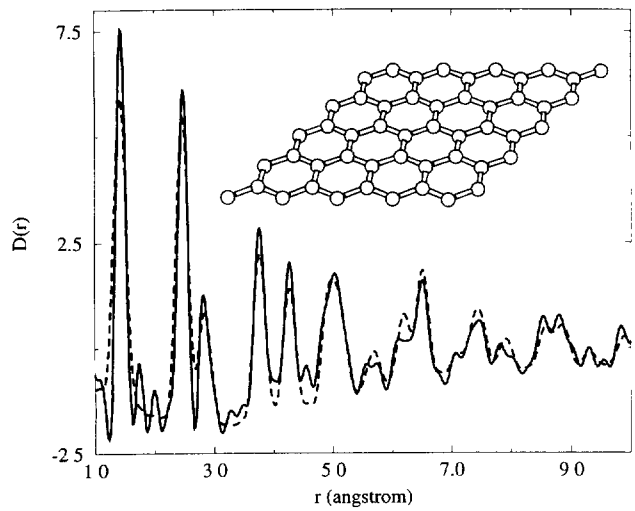

Fig. 3. Comparison between the calculated $D(r)$ of (· · ·) an isolated graphene fragment and (——) the data from ENR1000. The graphene particle is shown in the inset

apparent in the RDF, indicating that the layer stacking (which is evident from non-vanishing (002) Bragg intensity) is random parallel to the graphene fragments, an extreme example of turbostratic disorder.

3. Hydrogen effect

Amorphous carbons obtained by pyrolyzing organic solids at $T \leq 700$ °C retain substantial residual hydrogen and exhibit surprisingly large Li capacities [3,7,8]. Furthermore, an empirical correlation between H content and 'excess' Li capacity has been established [3]. Using inelastic neutron scattering vibrational spectroscopy, we found that the H saturates dangling bonds on edge C of the finite-size graphene flakes described above, similar to what occurs in hydrogenated amorphous Si. A single H bonded to an otherwise two-coordinated edge carbon preserves the sp^2p_π hybridization, and thus the possibility of binding either a second H to give a methyl moiety, or Li which, if occurring on neighbor pairs of edge C, would be analogous to the hypothetical organolithium molecule $C_2H_2Li_2$ [9]. The latter hypothesis has been confirmed by semi-empirical computer simulations on model hydrocarbons; in particular, we find no evidence for stable epitaxial Li_2 molecules [7] nor for large-scale occupancy of first-neighbor hexagons by intercalated Li.

Molecular vibrational spectroscopy based on inelastic neutron scattering offers several advantages relative to the more familiar infrared (IR) and Raman spectroscopies, in particular very high sensitivity to modes involving H motion (due to the huge incoherent thermal neutron cross section of the proton), and the absence of symmetry selection rules such that all modes are detectable. We used the reactor-based filter-analyzer neutron spectrometer (FANS) at NIST [10] to measure the vibrational densities of states of graphite and the two prototype epoxy-based carbons described above. The top panel of Fig. 4 shows spectra for ENR650 (closed circles) and ENR1000 (closed squares) at 16 K. Intense features in the former at 110 and 126 meV are assigned to out-of-plane vibrations of C–H species, with neighboring H's vibrating in-phase and out-of-phase, respectively. The broad maximum at 150 meV originates from C–H in-plane vibrations. These are also observable in ENR1000 but with much weaker intensities, and are (sensibly) absent in graphite. The lower panel of Fig. 4 shows calculated spectra based on semi-empirical potentials for a planar 7-hexagon graphene fragment with each edge C terminated by a single proton (coronene, solid curve) or 2 protons (dashed curve). The experimental results are clearly in better agreement with the former, confirming that we have single H saturation of dangling bonds at edge carbons. Disordered carbons obtained by low-temperature pyrolysis of organic precursors can therefore be reasonably modelled as a distribution of large polyaromatic hydrocarbons.

Addition of Li to these C–H entities would induce a downshift of the mode frequencies relative to the $C–H_2$ simulation since Li is heavier than H. We modelled the stability of C–H–Li species using semi-empirical quantum chemical methods, validated for small systems by ab initio LDA and quantum MD [1]. An example is shown in Fig. 5. The hexagons in pyrene $C_{16}H_{10}$ are terminated by either 2 or 3 hydrogens ('2H' and '3H'). Regardless of starting configuration, a single Li always relaxes to a position approximately cen-

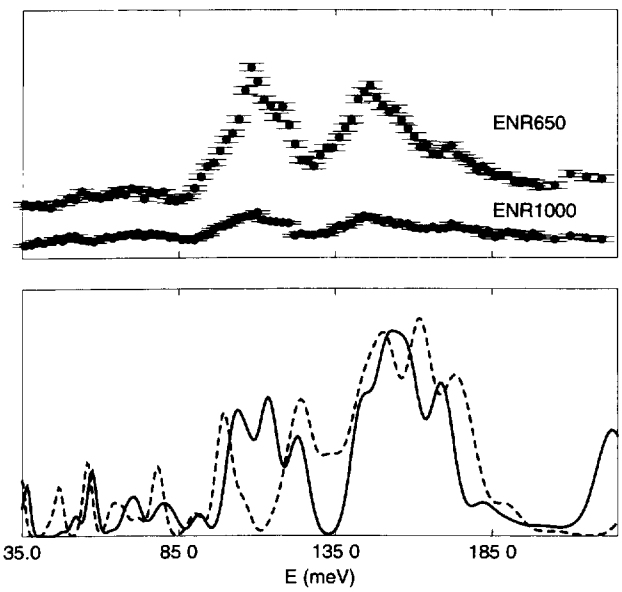

Fig. 4. Top: (●) vibrational densities of states for ENR650 and (■) ENR1000. Bottom: calculated spectra for a 7-hexagon graphene fragment with edge carbons terminated by (——) 1H or (· · ·) 2H

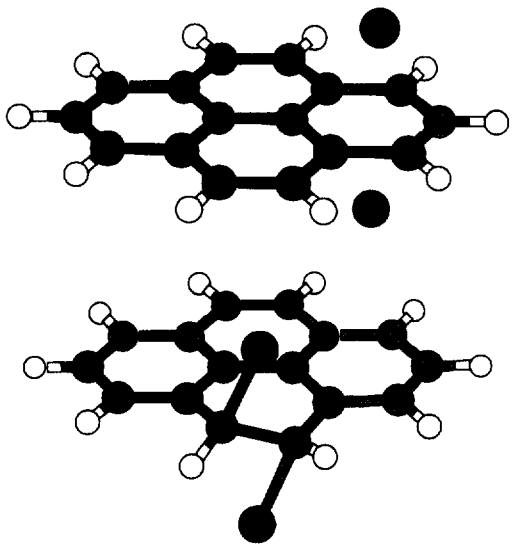

Fig. 5. Relaxed structures obtained by adding 2 Li's to $C_{16}H_{10}$ on opposite sides of the molecule centered over (top) 3H and (bottom) 2H rings.

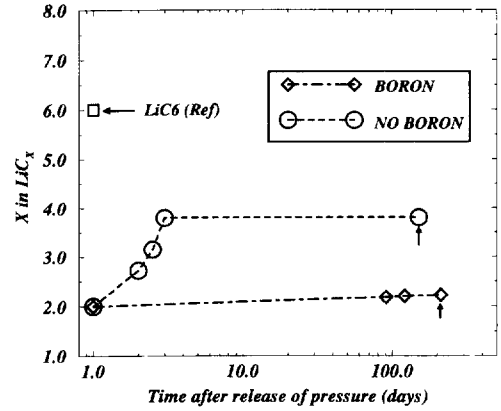

Fig. 6. Time dependence of x in high pressure-synthesized LiC_x, measured in days after releasing the pressure: (○) sample prepared from ordinary HOPG and (◇) sample prepared from HOPG containing 0.5 at.% boron. Horizontal arrow indicates LiC_6 for reference.

tered above 2H (88.7 kcal/mol) or 3H (85.3 kcal/mol). Two Li's initially above and below a 3H remain stable (Fig. 5 top), while when started above and below a 2H, they move off the interstitial sites and bond to the peripheral H-terminated carbons (Fig. 5 bottom). This requires sp^3 hybridization of both carbons (C–C bond length = 1.52 Å), and destroys the conjugation of that particular aromatic ring (1,2-bis-localization). Energy differences between interstitial and (C,H)-bonded Li's are insignificant. We therefore expect both to exist in real materials at similar potentials, strongly suggesting that residual hydrogen in low-temperature pyrolyzed amorphous carbons provides a second mechanism for Li uptake which operates in parallel with intercalation of Li into interstitial sites. Similar results are found for larger model hydrocarbons. By adding Li's sequentially to a large polyaromatic hydrocarbon and fully relaxing the intermediate structures, we find that Li's first occupy all available H-terminated edge sites which meet the criteria described above, then go to second-neighbor intersititial sites as in bulk LiC_6, and finally begin to form isolated Li clusters. At no point do we find stable epitaxial Li_2 molecules [7] nor Li multilayers [8].

4. Stabilizing LiC_2

High-pressure reactions of Li with graphite yield LiC_2, three times as dense in Li as the usual LiC_6 [11]. LiC_2 decomposes rapidly but incompletely into $LiC_6 + Li$ upon releasing pressure. We observe a dramatic enhancement in the (meta)stability when the graphite contains 0.5 at.% substitutional boron [2]. Average compositions derived from X-ray (OOL) intensities, determined several months after releasing the pressure, are $LiC_{2.2}$ and $LiC_{3.8}$ with and without boron respectively, as shown in Fig. 6. The origin of this phenomemon is not known. Boron is an acceptor in graphite, depressing the Fermi energy and increasing the electron affinity. But it is hard to believe that 1 boron per 200 carbons could have such a marked effect on the Li uptake by an electronic mechanism [12]. We speculate as follows. The metastable composition $LiC_{2.2}$ with boron is close to that of $Li_{27}C_{72}$, one of the intermediate decomposition products [11]. Further decomposition requires long-range Li diffusion. Since the volume per boron impurity is within a factor of ~2 of this unit cell volume, we suggest that boron arrests the decomposition cascade by pinning this metastable superlattice with ~1 boron per cell. It may be possible to exploit this metastability in the design of metal-free high capacity primary batteries.

Acknowledgements

This work was supported by the Hughes Electronics Co., the US Department of Energy under Grant No. DE-FC02-86ER45254, and by the National Science Foundation MRL Program under Grant No. DMR91-20668. We are grateful to T. Zheng and J. Dahn for providing the novolac-derived samples, and to D. Price, K. Volin and W.A. Kamitakahara for experimental assistance.

References

[1] P. Papanek, M. Radosavljević and J.E. Fischer, *Chem. Mater.*, 8 (1996) 1519.
[2] V.A. Nalimova, C Bindra and J.E. Fischer, *Solid State Commun.*, 97 (1996) 583
[3] J.R. Dahn, T. Zheng, Y. Liu and J.S. Xue, *Science*, 270 (1995) 590

[4] B.E. Warren, *X-ray Diffraction*, Addison–Wesley, New York, 1969
[5] R.K. Crawford, D.L Price, J.R. Haumann, R. Kleb, D G. Montague, J.M. Carpenter, S. Susman and R.J. Dejus, *Proc. 10th Meet. Advanced Neutron Sources*, Institute of Physics, Vol 97, IOP, New York, 1989, p. 419.
[6] D. Guerard and A. Herold, *Carbon, 13* (1975) 337.
[7] K. Sato, M. Noguchi, A. Demachi, N. Oki and M Endo, *Science, 264* (1994) 556.
[8] R. Yazami and M. Deschamps, *J Power Sources, 54* (1995) 411.
[9] U. Rothlisberger and M.L. Klein, *J. Am. Chem. Soc., 117* (1995) 42.
[10] R R. Cavanagh, J.J. Rush and R.D. Kelley, in J.T. Yates and T.E. Madey (eds.), *Vibrational Spectroscopy of Molecules on Surfaces*, Plenum, New York, 1987, p. 183.
[11] V.V. Avdeev, V.A. Nalimova and K.N. Semenenko, *High Pressure Res., 6* (1990) 11.
[12] B.M. Way and J R. Dahn, *J. Electrochem Soc., 141* (1994) 907.